Effects of CO_2 Degassing on pH and Fe(II) Oxidation Rates in Coal Mine Effluents

C. A. Cravotta III[1], J. N. Geroni[2]

[1]*U.S. Geological Survey Pennsylvania Water Science Center, 215 Limekiln Road, New Cumberland, PA 17070, USA*
[2]*Cardiff School of Engineering, Cardiff University, Queen's Buildings, The Parade, Cardiff, CF24 3AA, UK*

Abstract Elevated concentrations of dissolved CO_2 in groundwater from underground coal mines can depress pH and decrease the rate of removal of dissolved Fe(II) and associated metals within aerobic treatment ponds and wetlands. Mechanical aeration of the water can accelerate CO_2 removal (degassing), with consequent increases in pH and the rates of Fe(II) oxidation and Fe(III) precipitation. This paper uses kinetics modeling with the geochemical program, PHREEQC, to simulate interdependent changes in CO_2 degassing, pH, and Fe(II) oxidation rates that occur during aeration of waters discharged from abandoned coal mines.

Keywords abandoned mines; coal mine drainage; iron oxidation rate CO_2 degassing rate

Introduction

Concentrations of dissolved Fe(II) and CO_2 commonly are elevated in groundwater from coal mines (Kirby and Cravotta 2005). The elevated concentrations of dissolved CO_2 can be produced by reaction of acidic water with limestone or the oxidation of organic carbon (Langmuir 1997). Dissolved CO_2 will depress pH as indicated by the following reactions:

$$CO_2 + OH^- \rightarrow HCO_3^- \quad (1)$$

$$CO_2 + H_2O \rightarrow HCO_3^- + H^+ \quad (2)$$

Aeration of coal-mine effluent can promote CO_2 degassing and lead to an increase in pH (reverse of Eqs. 1 and 2) and an increase in Fe(II) oxidation rates (Cravotta 2007; Kirby *et al.* 2009; Geroni *et al.* 2012). This paper uses geochemical equilibrium and kinetics modeling with the geochemical program, PHREEQC (Parkhurst and Appelo 1999), to simulate interdependent changes in CO_2 degassing, pH, and Fe(II) oxidation rates during aeration of waters discharged from abandoned coal mines to treatment ponds or wetlands as reported in greater detail by Geroni *et al.* (2012).

Methods

Empirical time-series data on pH, temperature, dissolved oxygen (DO), and initial and final Fe(II) and alkalinity values during mechanical aeration experiments reported by Geroni *et al.* (2012) were used to estimate rates of Fe(II) oxidation and CO_2 degassing. Because the values for these unstable constituents changed rapidly, the mechanical aeration experiments were conducted for 2 hours or less. As previously described by Kirby *et al.* (2009), alkalinity was assumed to be consumed by the combined oxidation and hydrolysis of dissolved iron according to the stoichiometry:

$$Fe^{2+} + 2\,HCO_3^- + \tfrac{1}{2}\,H_2O + \tfrac{1}{4}\,O_2 \rightarrow Fe(OH)_3 + 2\,CO_2 \quad (3)$$

Rates of Fe(II) oxidation were estimated to follow the abiotic homogeneous oxidation rate model presented by Stumm and Morgan (1996, 683–685):

$$-d[Fe(II)]/dt = k_1 \cdot [O_2] \cdot [OH^-]^2 \cdot [Fe(II)] \quad (4)$$

where at pH > 5 and 20 °C, $k_1 = 8 \times 10^{13}$ M^{-2} atm^{-1} min^{-1} (1.33×10^{12} M^{-2} atm^{-1} s^{-1}). The second-order dependence on $[OH^-]$ indicates a

change in pH of 1 unit results in a 100-fold change in the oxidation rate. At a given pH, the rate increases by a factor of 10 for a 15 °C increase. By using the activation energy of 23 kcal/mol reported by Stumm and Morgan (1996, p. 684) with the Arrhenius equation (Langmuir 1997, p. 62), the rate can be adjusted to different temperatures.

A spreadsheet based 4th order Runge-Kutta (RK4) model was used to compute the concentration of residual Fe(II) with elapsed time based on Eq. (4). Values input into the model were initial Fe(II) concentration, along with the pH, temperature, and DO for each 10-second interval logged throughout the experiments. The apparent value for the homogeneous Fe(II) oxidation rate constant (k_1^* = 1.33 × 10^{12} to 1.33 × 10^{14} $M^{-2}atm^{-1}$ s^{-1}) was chosen to yield the residual Fe(II) at the end of the experiment. These apparent rate constants were a factor of 1 to 100 times the reference value of 1.33 × 10^{12} $M^{-2}atm^{-1}$ s^{-1} at 20 °C (Stumm and Morgan 1996, p. 683).

To facilitate the evaluation of the interactions among the initial alkalinity, pH, and Fe(II) oxidation rate, the major carbonate speciation equations and thermodynamic constants from the PHREEQC data base (Parkhurst and Appelo 1999) were added to the spreadsheet RK4 model. The measured pH and temperature plus computed alkalinity (Eq. 3) were then used to estimate partial pressure of CO_2 (pCO_2) and the rate of CO_2 degassing during the aeration experiments considering asymptotic exponential models (Langmuir 1997; Geroni *et al.* 2012). The integrated form of the 2nd order asymptotic rate equation for CO_2 degassing is shown as Eq. (5),

$$t \cdot k_L a = [1/(C_S - C_t) + 1/(C_S - C_O)] \quad (5)$$

where C_S is the steady state (equilibrium) value, C_O is the initial value and C_t is the value at time t for the negative logarithm of pCO_2 in atmospheres (p_{CO_2}). Values for $-k_L a$ (the mass transfer coefficient) were calculated from the linear slope estimate of $[1/(C_S - C_t) + 1/(C_S - C_O)]$ *vs.* t over the first 10 to 25 minutes of the experiments. The value of C_S was varied to yield $k_L a$ that approximated the trend for pCO_2 (C_t) during each experiment. The modeled values of C_S ($pCO_2 = 10^{-3.4}$ to $10^{-1.7}$ atm) and $k_L a$ for the batch aeration experiments were consistent with previous studies indicating initially rapid CO_2 degassing and approach to a steady state that can be at disequilibrium with atmospheric pCO_2 ($10^{-3.4}$ atm; Cravotta 2007; Kirby *et al.* 2009).

The PHREEQC aqueous speciation model (Parkhurst and Appelo 1999) was used to couple the rate equations for CO_2 degassing and Fe(II) oxidation and calculate the corresponding changes in pH and concentrations of Fe(II), dissolved CO_2 species, and other aqueous ions, assuming spontaneous equilibrium with atmospheric O_2 and considering thermodynamic feasibility for precipitation of $Fe(OH)_3$. Initial values for pH, alkalinity, DO, and Fe(II) concentration and the average temperature during each CO_2 stripping experiment were input along with estimated $k_L a$ (calculated for the 2nd order rate equation) and apparent k_1 values (as used in the RK4 model) estimated by multiplying the reference k_1 value of 1.33 × 10^{12} $M^{-2}atm^{-1}$ s^{-1} at 20 °C (Stumm and Morgan 1996, p. 683) by a factor ranging from 0.1 to 100. Model calibration was conducted by adjusting the apparent $k_L a$ and k_1 values to obtain the best fit of measured data for logged pH (paired values) and measured alkalinity and Fe(II) at the beginning and end of each experiment.

Results and Discussion

Initial pH of discharges at all four sites before aeration was circumneutral (5.6 to 6.7); however, the effluents were either net-acidic, with positive hot acidity (Blenkinsopp, Tan-y-Garn, and Ynysarwed; Table 1), or net-alkaline, with negative hot acidity (Six Bells). After 2 hours of aeration and CO_2 stripping from the net acidic waters, the Fe(II) concentration decreased from greater than 40 mg/L to less than 6 mg/L while pH remained within 0.1 unit of the initial

Site	Pre aeration					
	Hot Acidity (mg L^{-1} $CaCO_3$)	Cold Acidity (mg L^{-1} $CaCO_3$)	Alkalinity (mg L^{-1} $CaCO_3$)	pH	Fe(II) (mg L^{-1})	Temperature (°C)
Blenkinsop	33 to 55	423 to 476	264	5.6 to 6.0	137	13.4
Tan-y-Garn	16 to 22	177 to 186	57 to 58	5.6	41	12.2
Ynysarwed	29 to 33	259 to 280	143 to 146	5.8 to 5.9	93.7	13.9
Six Bells	-615	208 to 222	746 to 752	6.6 to 6.7	19	18.9
Site	Post aeration					
	Time elapsed (min)	Cold Acidity (mg L^{-1} $CaCO_3$)	Alkalinity (mg L^{-1} $CaCO_3$)	pH	Fe(II) (mg L^{-1})	Temperature (°C)
Blenkinsop	115	21 to 23	34 to 38	5.5 to 5.9	5.75	17.75
Tan-y-Garn	115	16 to 19	1	5.5 to 6.0	4.3	18.0
Ynysarwed	127	45 to 51	5 to 7	5.7 to 5.8	2.79	18.3
Six Bells	28	0	618 to 631	8.4	0.05	20.0

***Table 1**. Comparison of measured hot acidity, cold acidity, alkalinity, pH, Fe(II) content, and temperature of water at the beginning and end of the batch-wise CO_2 stripping experiments*

Site	k_1 factor $k_1 = 1.33 \times 10^{12}$ RK4		$k_{1*} \times 10^{12}$ at 20 °C (M^{-2} atm^{-1} s^{-1})	Alk_0 (mg L^{-1})	C_o -log pco_2	C_s -log pco_2	k_La (log(atm)$^{-1}$ s^{-1})	Equilibrium assumption
	PHREEQCi models							
Blenkinsopp	64 to 70	40	94	250	0.40	2.0	0.001279	O_2; $Fe(OH)_3$
Tan-y-Garn	22 to 23	20	47	70	0.80	2.8	0.000426	O_2; $Fe(OH)_3$
Ynysarwed	90 to 100	50	107	165	0.64	2.8	0.000203	O_2; $Fe(OH)_3$
Six Bells	1 to 3.4	1	1.5	749	0.77	3.1	0.000933	O_2; $Fe(OH)_3$;$CaCO_3$

For PHREEQC models, initial pH, Fe(II), and alkalinity values and average temperature for batch aeration tests defined the starting solution. Apparent oxidation rate constant, k_1^*, for Eq. (4) indicated by k_1 factor multiplied by 1.33×10^{12} M^{-2} atm^{-1} s^{-1}. Apparent rate constant corrected to 20 °C using Arhhenius equation (Langmuir 1997, p. 62), with activation energy of 23 kcal/mol (Stumm and Morgan 1996). Exchange with atmospheric oxygen ($PO_2 = 10^{-0.27}$ atm) and precipitation of $Fe(OH)_3$ to SI< 0 were specified to maintain equilibrium. For calibrated Six Bells models, precipitation of calcite after supersaturation was considered to maintain $SI_{CALCITE} < 1.0$.

***Table 2**. Values of constants and associated variables used in RK4 model of Fe(II) oxidation and calibrated PHREEQCi kinetics models of CO_2 degassing and Fe(II) oxidation*

value (Table 1). In contrast, after only 30 minutes of aeration of the net-alkaline water, Fe(II) decreased from 19 mg/L to less than 0.1 mg/L and pH increased by almost 2 units (Table 1). The pH of net acidic waters increased initially because of rapid CO_2 degassing and then decreased because of protons released by Fe(III) hydrolysis (Figs. 1a – 1c), whereas the pH of the net alkaline water increased progressively during aeration (Fig. 1d). The rapid increase in pH during early stages of aeration of all the waters coincided with an asymptotic decrease in the dissolved CO_2 from initial pco_2 values of $10^{-0.4}$ to $10^{-0.8}$ atm to estimated steady-state values ranging from $10^{-1.7}$ to $10^{-3.4}$ atm (Figs. 1 and 2).

Figs. 1 and 2 show the measured pH, Fe(II), alkalinity, and pco_2 and the PHREEQC simulated values produced by coupling the rate equations for CO_2 degassing and Fe(II) oxidation. Fig. 1 shows the paired values of measured pH as subparallel dotted curves and corresponding estimates of the pH by selected rate models as additional curves. The apparent Fe(II) oxidation rate corrected to 20 °C for the net acidic waters were 47 to 107 times the reference k_1 value at 20 °C, whereas that for the net alkaline water was 1.5 times the reference value (Table 2). Although these rates are within the range of reported homogeneous Fe(II) oxidation rates in mine waters (Geroni and Sapsford 2011), apparent k_1 factors greater than 1 may be attributed to heterogeneous oxidation by Fe(III) particles. We considered combined homogeneous and heterogeneous Fe(II) oxida-

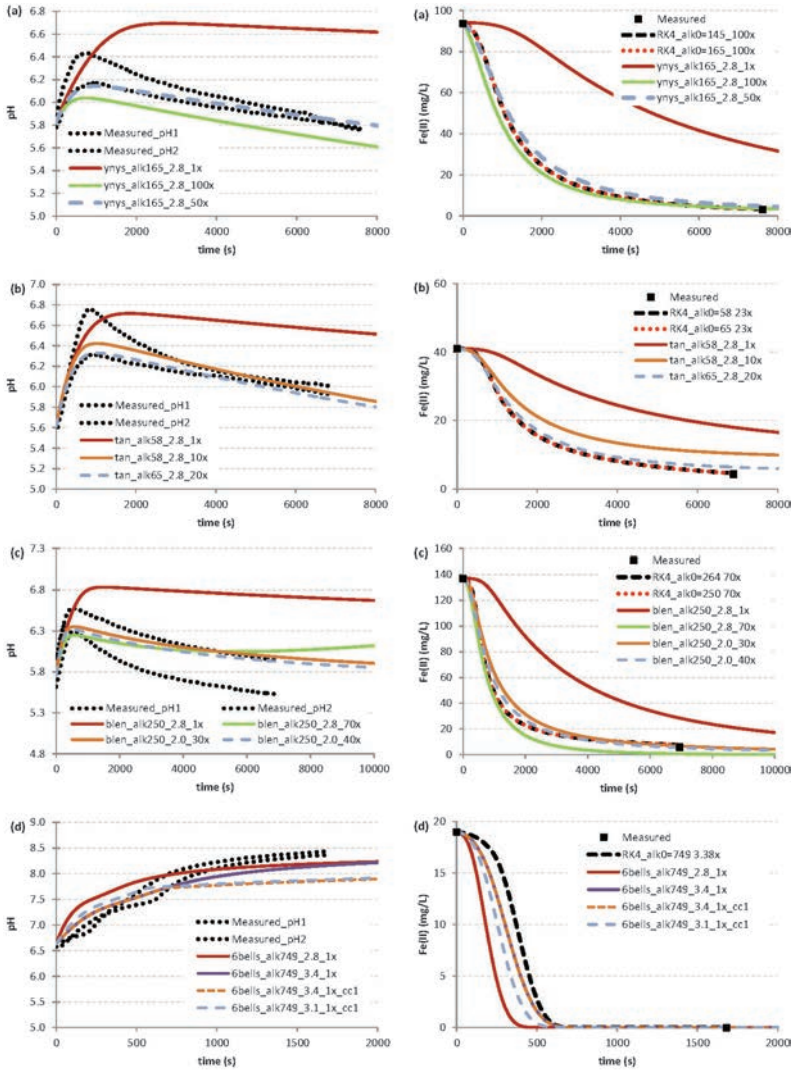

Fig. 1 *Comparison of measured pH and estimated Fe(II) concentrations from spreadsheet based RK4 model to simulated pH and Fe(II) from PHREEQC models (after Geroni et al. 2012): (a) Ynysarwed (ynys), (b) Tan-y-Garn (tan), (c) Blenkinsopp (blen), (d) Six Bells (6bells). Values for initial alkalinity and rate constants used for RK4 and PHREEQ models are summarized in Table 2. In legend, Alk_0 (58 to 749 mg/L $CaCO_3$ equivalent), steady-state pco_2 (2.0 to 3.4) and k_1 multiplication factor (1× to 90×) are given for each simulation. The unbroken red curve indicates the reference simulation for values of $k_1 = 1.33 \times 10^{12}$ $M^{-2}atm^{-1}s^{-1}$ and steady-state $pco_2 = 2.8$. Dashed curves show results for calibrated models; for Six Bells, calcite precipitation maintained $SI_{CALCITE} < 1$ (cc1).*

tion rate equations (*e.g.* Dempsey *et al.* 2001) as an alternative model for the PHREEQC simulations. However, the inclusion of heterogeneous oxidation did not improve our ability to simulate the empirical results. By adjusting only the apparent rate constants for homogeneous Fe(II) oxidation and CO_2 degassing, the observed pH, Fe(II), and alkalinity data could be simulated. For refinement of the Tan-y-Garn and Ynysarwed models, the starting alkalinity values were increased from 58 to 70 mg/L and 148 to 165 mg/L, respectively, and for the Six Bells model, precipitation of calcite was simulated upon reaching supersaturation ($SI_{CALCITE} < 1.0$). After calibration, simulated values for pH were within the range of measured values, and simulated values for Fe(II) and alkalinity were comparable to those at the beginning and end of the experiments (Figs. 1 and 2).

Conclusions

Elevated concentrations of dissolved CO_2 in effluent from underground coal mines can depress pH and decrease the rate of removal of dissolved Fe(II) within aerobic treatment ponds and wetlands. Aeration of the effluent can accelerate CO_2 removal (degassing) and increase pH, with a consequent increase in the rate of Fe(II) oxidation and Fe(III) precipitation.

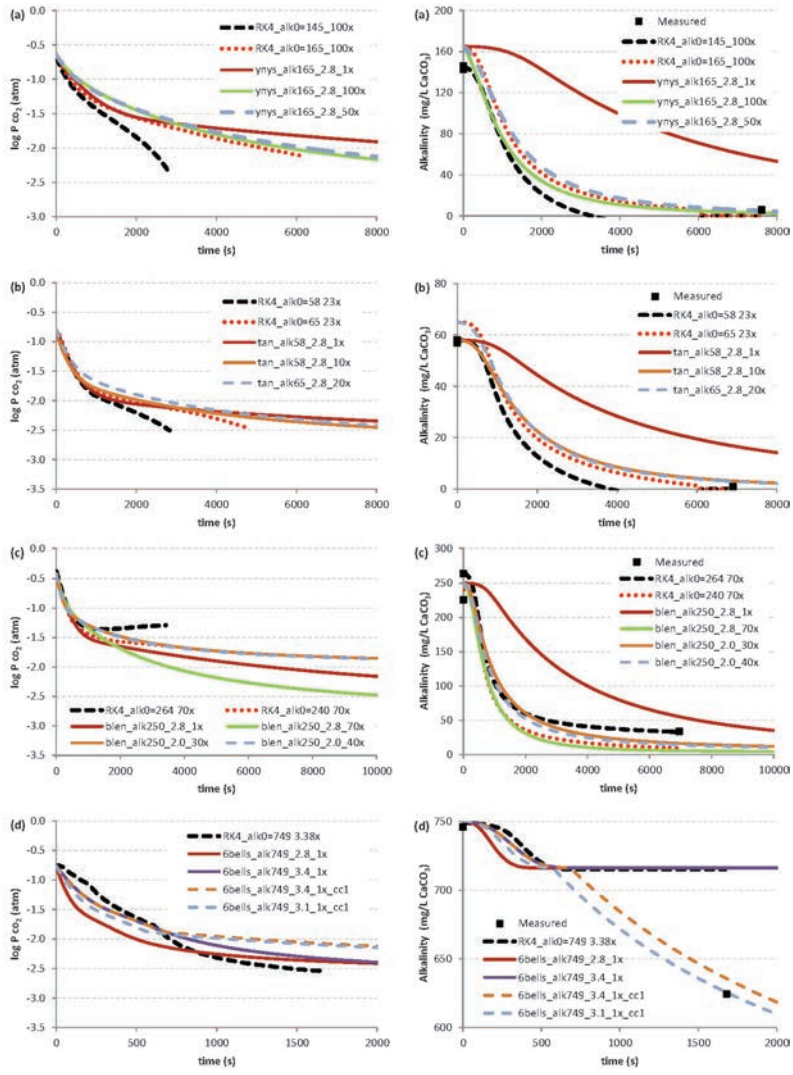

Fig. 2 *Comparison of estimated pco_2 and alkalinity concentrations from spreadsheet based RK4 model to simulated pco_2 and alkalinity from PHREEQC models: (a) Ynysarwed; (b) Tan-y-Garn; (c) Blenkinsopp; (d) Six Bells. Values for initial alkalinity and rate constants used for RK4 and PHREEQ models are summarized in Table 2. In legend, Alk_0 (58 to 749 mg/L $CaCO_3$ equivalent), steady-state pco_2 (2.0 to 3.4) and k_1 multiplication factor (1x to 90x) are given for each simulation. The unbroken red curve indicates the reference simulation for values of $k_1 = 1.33 \times 10^{12}$ $M^{-2}atm^{-1}s^{-1}$ and steady-state $pco_2 = 2.8$. Dashed curves show results for calibrated models; for Six Bells, calcite precipitation maintained $SI_{CALCITE} < 1$ (cc1).*

The rate of CO_2 degassing during mechanical aeration experiments was successfully described using a 2nd order asymptotic exponential model and that for Fe(II) oxidation was described using a 1st order exponential rate model for homogeneous oxidation. Because the homogeneous rate model for Fe(II) oxidation is strongly dependent on the pH, the rate of CO_2 degassing was a major factor affecting the rate of Fe(II) oxidation. With the PHREEQC modeling approach, the pH was permitted to change with reaction progress and was controlled primarily by the rate of CO_2 degassing and secondarily by the extent of Fe(III) hydrolysis and the available alkalinity. The empirical data and associated simulations indicated that hydrolysis of Fe(III) depressed the pH of net acidic water to a greater extent than that of net alkaline water. Although the rates of Fe(II) oxidation for the net acidic effluents were 47 to 107 times the reference k_1 value at 20 °C, the Fe(II) oxidation and removal rates were slower for net acidic effluents than for the net alkaline effluent.

The measured trends in pH and Fe(II) concentrations during aeration experiments demonstrated potential for pH to affect Fe(II) oxidation rate in accordance with the homogeneous oxidation rate model. Despite limited availability and quality of the time-series data,

kinetics modeling using the geochemical speciation program, PHREEQC, provided insight into the interactions among chemical processes and the relative importance of specific reactions, such as CO_2 degassing, Fe(III) hydrolysis, and calcite precipitation, on the pH of poorly buffered water. Empirical data on temperature, DO, pH, alkalinity, Fe(II) concentration, and associated solutes and solids generally are needed to estimate the kinetics of CO_2 degassing and Fe(II) oxidation during aeration tests or within treatment systems. With this information, treatment strategies can be evaluated to optimize the removal of Fe(II) while minimizing the use of chemicals for pH adjustment.

References

Cravotta CA III (2007) Passive aerobic treatment of net-alkaline, iron laden drainage from a flooded underground anthracite mine, Pennsylvania, USA. Mine Water Environ. 26, 128–149

Dempsey BA, Roscoe HC, Ames R, Hedin R, Jeon B-H (2001) Ferrous oxidation chemistry in passive abiotic systems for the treatment of mine drainage. Geochem. Explor. Environ. Anal. 1, 81–88

Geroni JN, Sapsford DJ (2011) Kinetics of iron (II) oxidation determined in the field. Appl. Geochem. 26, 1452–1457

Geroni JN, Cravotta CA III, Sapsford DJ (2012) Evolution of the chemistry of Fe bearing waters during CO_2 degassing. Appl. Geochem. 27, 2335–2347

Kirby, CS, Cravotta CA III (2005) Net alkalinity and net acidity 2: Practical considerations. Appl. Geochem. 20, 1941–1964

Kirby CS, Dennis A, Kahler A (2009) Aeration to degas CO_2, increase pH, and increase iron oxidation rates for efficient treatment of net alkaline mine drainage. Appl. Geochem. 24, 1175–1184

Langmuir D (1997) Aqueous environmental geochemistry. Prentice Hall, New Jersey, USA, 600 p

Parkhurst DL, Appelo CAJ (1999) User's guide to PHREEQC (Version 2)—A computer program for speciation, batch-reaction, one-dimensional transport, and inverse geochemical calculations. U.S. Geol. Surv. Water-Resour. Inv. Re99–4259, 310 p

Stumm W, Morgan JJ (1996) Aquatic chemistry—chemical equilibria and rates in natural waters (3rd). New York, Wiley-Interscience 1022 p